INTERNATIONAL JOURNAL FOR NUMERICAL METHODS IN FLUIDS
Int. J. Numer. Meth. Fluids 2005; **47**:1353–1359
Published online 29 December 2004 in Wiley InterScience (www.interscience.wiley.com). DOI: 10.1002/fld.839

Finite element simulation of three-dimensional free-surface flow problems with dynamic contact lines

M. A. Walkley[1*,†], P. H. Gaskell[2], P. K. Jimack[1], M. A. Kelmanson[3] and J. L. Summers[2]

[1]*School of Computing, University of Leeds, Leeds, LS2 9JT, U.K.*
[2]*School of Mechanical Engineering, University of Leeds, Leeds, LS2 9JT, U.K.*
[3]*Department of Applied Mathematics, University of Leeds, Leeds, LS2 9JT, U.K.*

SUMMARY

An arbitrary Lagrangian–Eulerian (ALE) finite element method is described for the solution of three-dimensional free-surface flow problems. The focus of this work is on extending the algorithm to include a dynamic contact line model allowing the fluid free surface, in the steady case, to form a prespecified static contact angle with a solid boundary and, in the transient case, to move along the solid boundary. This widens the applicability of the algorithm to important industrial applications such as forced spreading of fluids and gravity-driven flow on inclined surfaces. Copyright © 2004 John Wiley & Sons, Ltd.

KEY WORDS: finite element method; free-surface flow; surface tension; dynamic contact lines

1. INTRODUCTION

Free-surface flow problems occur in a wide variety of scientific and engineering applications. Examples include phase-change problems, coating flows, the spreading of viscous fluids and the motion of drops or bubbles. The primary interest of this paper is the development of a numerical technique for the simulation of time-dependent free-surface flows in three dimensions, which represents one of the most important practical computational challenges for this class of problem. The requirement for time dependence is apparent in almost all applications since understanding the evolution and stability of free surfaces provides one of the major incentives for their mathematical and computational study. Furthermore, fully three-dimensional simulations are required in order to capture all of the physically important features of most free-surface flows. For example, the forced spreading of a fluid droplet on a chemically or

*Correspondence to: M. A. Walkley, School of Computing, University of Leeds, Leeds, LS2 9JT, U.K.
†E-mail: markw@comp.leeds.ac.uk

Contract/grant sponsor: EPSRC; contract/grant number: GR/R25453/01

Received 27 April 2004
Revised 10 August 2004
Accepted 17 August 2004

topologically patterned surface, a problem with significant practical interest in the context of coating flows [1], is necessarily both time-dependent and three-dimensional. In recent years there has been a significant interest in the computational study of such flows using ALE finite element methods, e.g. References [2, 3], and it is this approach that is pursued here.

The numerical technique described in this paper is an extension of the three-dimensional algorithm introduced in Reference [4]. The principal aim of the paper is to provide a three-dimensional incompressible free-surface flow solver based upon the use of implicitly stable elements (the so-called Taylor–Hood element); to represent the three-dimensional free surface using piecewise quadratics for optimal accuracy with the chosen elements (this is of particular significance when surface-tension effects are dominant), and; to implement the three-dimensional moving-mesh algorithm in conjunction with a discrete mesh regeneration procedure (to allow for larger geometry changes to occur than is otherwise possible). Particular attention is paid to the modelling of the contact line, where the fluid free surface meets a solid surface. The previous model is extended so that for steady flows a given static contact angle between these two surfaces can be achieved. For time-dependent flows a dynamic contact angle model is implemented which allows motion of the free surface along a solid boundary.

The complete method is demonstrated through a range of examples. The necessity to include a static contact angle at a contact line is illustrated through modelling the gravity-driven spreading of a fluid droplet and the formation of a meniscus in a cylindrical container. The motion of a fluid droplet on an inclined plane applies the model to a problem with a dynamic contact line. The paper concludes with a brief discussion of the strengths and current limitations of the work.

2. MATHEMATICAL MODEL

The problem to be modelled can be described by the three-dimensional Stokes equations for velocity field $\mathbf{u}$ and pressure p, written in the following non-dimensional form:

$$\mathbf{0} = \nabla \cdot \boldsymbol{\sigma} + St\mathbf{f}, \quad 0 = \nabla \cdot \mathbf{u} \tag{1}$$

where $\boldsymbol{\sigma} = -p\mathbf{I} + \nabla\mathbf{u} + \nabla\mathbf{u}^{\mathrm{T}}$ is the stress tensor, $\mathbf{f}$ is the exterior force and St is the Stokes number. The fluid domain Ω is assumed to be simply connected and is bounded by either a fluid free surface Γ_f or a solid wall Γ_w. The contour defined by the interface of these two surfaces is termed the contact line γ_c. On the solid boundary Γ_w a no-slip condition is applied and, at the free surface Γ_f the following kinematic condition and stress condition are applied:

$$\mathbf{n}_f \cdot (\mathbf{u} - \dot{\mathbf{x}}_f) = 0, \quad \mathbf{n}_f \cdot \boldsymbol{\sigma} = -\mathbf{n}_f p_{\mathrm{ext}} + \frac{1}{Ca}\left(\nabla_S \cdot \mathbf{n}_f\right)\mathbf{n}_f \tag{2}$$

In (2) $\mathbf{n}_f$ represents the outward normal to the free surface whose location is given by $\mathbf{x}_f$, the dot above a variable denotes its time derivative, $\mathbf{u}$ represents the fluid velocity at a point on the free surface, p_{ext} is the external pressure, which may be taken as zero for simplicity, $\nabla_S = (\mathbf{I} - \mathbf{n}_f\mathbf{n}_f) \cdot \nabla$ is the surface gradient operator and Ca is the capillary number which is inversely proportional to surface tension (which is assumed to be constant over the entire free surface).

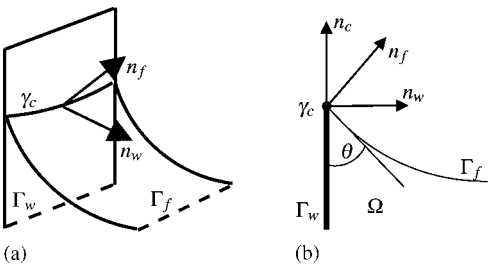

Figure 1. Geometrical description of the contact line: (a) 3d model; and (b) 2d section in the plane of $\mathbf{n}_w$ and $\mathbf{n}_f$.

In previous work by the authors [4] it was assumed that the contact line γ_c was fixed and the no-slip condition was applied there. In effect there was no restriction on the angle formed between the fluid free surface and the solid boundary. This is appropriate for some flows, for example the development of a fluid droplet from a pipette, but clearly there are cases, such as the modelling of a fluid meniscus, where it is desirable to specify a static contact angle, θ_s, on this boundary. The value of θ_s is determined *a priori* by properties of both the fluid and the solid surface and can be given as a physical parameter of the problem. In a more general framework the contact line is allowed to move forming a dynamic contact angle, θ, between the fluid and solid surfaces. Figure 1 depicts the geometry of the contact line on which the model is based. In practice $\mathbf{n}_f$ and $\mathbf{n}_w$ (the outward normal to the solid boundary) are computed from the current geometry whilst $\mathbf{n}_c$, the tangent to the solid surface in the plane of $\mathbf{n}_f$ and $\mathbf{n}_w$, defines locally the direction in which the free surface is allowed to move. Strictly, this problem cannot be uniquely defined within the Stokes flow framework since the contact line is both part of the solid boundary, which is subject to the no-slip condition, and the fluid boundary, which is subject to the kinematic condition. Detailed mathematical analyses of this problem and alternative mathematical models appear in the literature, e.g. References [5, 6]. In general these models may be expressed in the form

$$\mathbf{n}_w \cdot \mathbf{n}_f = \cos(\theta) = f(\theta_s, \dot{x}_c) \tag{3}$$

with the precise definition of $f(\theta_s, \dot{x}_c)$ determined by the selected model. Equation (3) may be used to compute the local speed of the contact line $\dot{x}_c$ in the direction $\mathbf{n}_c$. The specific model used in this paper is taken from Reference [7] and has previously been applied in three dimensions by Baer *et al.* [2]:

$$f(\theta_s, \dot{x}_c) = \cos(\theta_s) - c_T \, Ca \, \dot{x}_c \tag{4}$$

The constant c_T in this model is arbitrary and an appropriate value should be determined empirically to scale the contact line speed relative to the dynamic contact angle. It is straightforward to include this general model of the contact line in the current algorithm, as is described in the following section.

3. NUMERICAL MODEL

The system of equations described in the previous section represent a time-dependent, non-linear flow in which the spatial domain evolves with the problem. The computational algorithm used here has been described in detail in Reference [4]. In previous work, e.g. Reference [2], this problem has been solved in a fully coupled fashion, however here the flow solution is decoupled from the boundary motion at each time step in the following manner. First, solve the steady Stokes equations to compute the pressure and velocity field. Second, update the free surface position Γ_f using the computed velocity. The contact line model (3), which prescribes the motion of the mesh nodes on γ_c, is incorporated at this stage. Finally, adapt the interior mesh through a pseudo-elastic solid motion of the mesh points, subject to displacements enforced by the free-surface displacement.

Other distinguishing features of the model presented here, compared to previous work, are: the use of an *a priori* LBB stable Taylor–Hood finite element method for the Stokes problem, using isoparametric quadratic tetrahedral elements; an isoparametric quadratic triangular model of the free surface, allowing an accurate representation of the free-surface curvature and hence the associated surface tension forces; the use of both continuous adaptivity, in the form of mesh movement, and discrete remeshing, allowing large deformations of the fluid domain.

Mesh movement is driven by the deformation of the fluid free surface due to the kinematic boundary condition. The interior mesh is adapted at each time step by a pseudo-linear elastic displacement. This linear elastic problem is discretized using a linear finite element method and solved with a Gauss–Seidel iterative technique [4]. In general two iterations are sufficient to produce a satisfactory evolution of the interior mesh. However, mesh movement is only effective if the fluid volume does not change significantly, the domain does not distort significantly and the free surface mesh quality is maintained. In cases where these conditions do not apply it is also necessary to discretely remesh the whole domain. The quality of the existing mesh is monitored through the integral of the curvature on the mesh edges: $I_\kappa = \int_s |\kappa| \, \mathrm{d}s$, where κ is the curvature [8], which can be computed directly as a piecewise constant on the locally quadratic edge. This measure indicates regions in which surface curvature is large relative to the local mesh resolution.

4. COMPUTATIONAL EXAMPLES

Examples are given of the algorithm applied to problems in which the solution evolves to a steady state, and also to a problem with a dynamic contact line whose motion is governed by our choice of contact line model. In all cases the initial meshing of the computational domain and the discrete remeshing stages are performed using the NETGEN software [9].

The first example comprises an initially hemispherical droplet, of radius 1, at Stokes number 1 and capillary number 1 on a solid, plane surface with gravity acting perpendicular to the plane. The initial mesh has 396 nodes and 179 elements. The computation is impulsively started from a dynamic contact angle $\theta = 90°$ and the droplet returns to its equilibrium position which is determined by the specified static contact angle θ_s. Figures 2(a)–(b) show two examples in which θ_s is set to 60 and 120°, respectively. In each case the spatial domain is remeshed once during the computation, triggered by the edge-curvature measure exceeding a given tolerance. In case (a) the final number of nodes and elements are 886 and 412 and

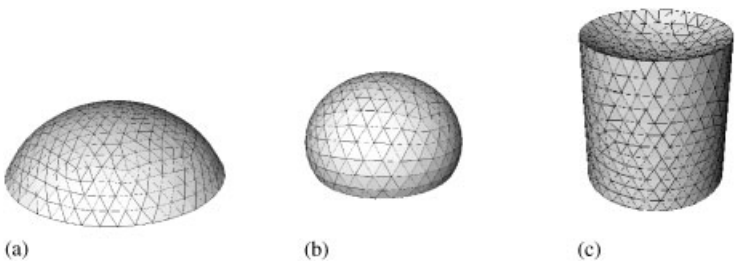

Figure 2. Computation to steady state with a specified static contact angle: (a) Droplet spreading $Ca = 1$, $St = 1$, $\theta_s = 60°$; (b) Droplet spreading $Ca = 1$, $St = 1$, $\theta_s = 120°$; and (c) Meniscus formation $Ca = 1$, $St = 1$, $\theta_s = 60°$.

Figure 3. Computation with a dynamic contact line: (a) $t = 0.1$; (b) $t = 10.0$; and (c) $t = 20.0$.

in case (b) 530 and 229, respectively. Note that in both cases the transient solution to the correct steady-state is computed and for case (a) the maximum droplet height is found to decay in proportion to $t^{-0.21}$, which is consistent with experimental and theoretical results reported elsewhere (e.g. Reference [10] and references therein).

In the second example fluid is confined by a cylindrical solid boundary of radius 0.5 with Stokes number 1, capillary number 1 and gravity acting along the axis of the cylinder. The initial mesh has 895 nodes and 450 elements. The computation is impulsively started from a dynamic contact angle of $\theta = 90°$ and evolves to a steady state with a specified static contact angle of 60° as shown in Figure 2(c). Discrete remeshing is not required here as the edge-curvature measure does not exceed the given tolerance.

The final example applies the algorithm to the gravity-driven motion of a fluid droplet on a plane inclined at 20° to the horizontal, with gravity acting vertically. The droplet is initially hemispherical with radius 1, the Stokes number and capillary number are both 1, implying a balance between capillary and gravitational effects, and the static contact angle $\theta_s = 90°$. The initial mesh has 396 nodes and 179 elements. The problem is started impulsively by rotating the gravitational body force to simulate the instantaneous inclination of the plane. Figure 3 shows the evolution of the droplet as it slides down the plane. The curvature of the surface increases at the front of the droplet and correspondingly decreases near the tail but the horizontal profile of the droplet remains approximately circular, probably due to the viscous nature of the Stokes flow modelled here. If the Stokes number is increased by a factor of 10 (or the capillary number correspondingly decreased) we see a similar flow evolution but with an enhanced steepening of the advancing edge as expected. Baer *et al.* [2] solved a similar problem, but at a non-zero Reynolds number, and reported significant evolution of the droplet shape, although their results are performed without remeshing and suffer from a lack of resolution at later times. Figure 4(a) shows the evolution of the edge-curvature

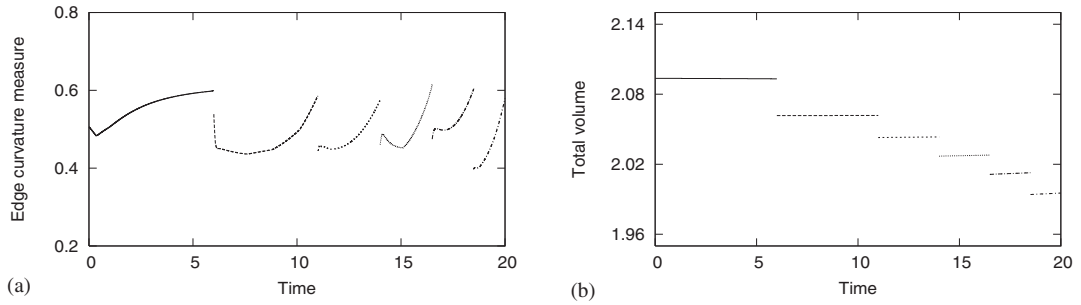

Figure 4. Statistics of the adaptive mesh procedure (a) Edge curvature measure; and (b) Fluid volume.

measure in time and the remeshing stages that are performed with a curvature threshold set to 0.6. The growth during the computation is attributed to the redistribution of free surface nodes from the front of the advancing droplet towards the rear, increasing the discrete edge curvature at the front of the droplet. Figure 4(b) depicts the evolution of the fluid volume during the computation. The overall mass loss represents approximately 4% of the initial fluid volume after 20 000 time steps. It is clear that almost all of this loss is attributed to the discrete remeshing stages, due to the interpolation of new mesh nodes onto the original piecewise-quadratic surface, and further work is required to minimise this source of mass loss.

5. DISCUSSION

An adaptive ALE finite element method for the solution of three-dimensional moving-boundary problems in the presence of dynamic contact lines has been described. By the use of isoparametric quadratic tetrahedral Taylor–Hood elements we are able to represent the geometry of the free surface, and hence the curvature-dependent surface-tension forces, to a higher degree of accuracy than has been possible with previously published three-dimensional models. In particular, when considering the implementation at the contact line, the model can accurately represent the required contact angles and surface curvature at a solid boundary. The mathematical model of the contact line is quite general but also rather simplistic. Alternative models [5, 6] are possible within the framework of Equation (3) and will be investigated and contrasted. This model can also be calibrated and validated by comparison with laboratory experiments. Further validation of the whole computational model will be obtained by comparison with numerical models describing thin-film evolution on topologically and chemically patterned surfaces [1, 11]. Potential future applications of the model include the industrially important process of spin coating.

REFERENCES

1. Gaskell PH, Jimack PK, Sellier M, Thompson HM. Efficient and accurate time adaptive multigrid simulations of droplet spreading. *International Journal for Numerical Methods in Fluids* 2004, to appear.
2. Baer TA, Cairncross RA, Schunk PR, Rao RR, Sackinger PA. A finite element method for free surface flows of incompressible fluids in three dimensions. Part II. Dynamic wetting lines. *International Journal for Numerical Methods in Fluids* 2000; **33**:405–427.

3. Zhou H, Derby JJ. An assessment of a parallel, finite element method for 3-d, moving-boundary flows driven by capillarity for simulation of viscous sintering. *International Journal for Numerical Methods in Fluids* 2001; **36**:841–865.
4. Walkley MA, Gaskell PH, Jimack PK, Kelmanson MA, Summers JL. Finite element simulation of three-dimensional free-surface flow problems. *Journal of Scientific Computing* 2004, to appear.
5. Shikhmurzaev YD. Moving contact lines in liquid/liquid/solid systems. *Journal of Fluid Mechanics* 1997; **334**:211–249.
6. Voinov OV. Wetting: Inverse dynamic problem and equations for microscopic particles. *Journal of Colloid and Interface Science* 2000; **226**:5–15.
7. Kistler SF. Hydrodynamics of wetting. In *Wettability*, Berg JC (ed). Marcel Dekker: New York, 1993; 311–429.
8. Struik DJ. *Differential Geometry* (2nd edn). Addison-Wesley: Reading, MA, 1961.
9. Schöberl J. NETGEN—An advancing front 2D/3D-mesh generator based on abstract rules. *Computing and Visualization in Science* 1997; **1**:41–52.
10. Schwartz LW, Eley RR. Simulation of droplet motion on low energy and heterogeneous surfaces. *Journal of Colloid and Interface Science* 1998; **202**:173–188.
11. Gaskell PH, Jimack PK, Sellier M, Thompson HM, Wilson MCT. Gravity-driven flow of continuous thin liquid films on non-porous substrates with topography. *Journal of Fluid Mechanics* 2004; **509**:253–280.

